NASA TECHNICAL NOTE

NASA TN D-4845

LOAN COPY: RETURN
AFWL (WLIL-2)
KIRTLAND AFB, N MEX

TECH LIBRARY KAFB, NM
0131623

NASA TN D-4845

EFFECTS OF EDGE CONSTRAINTS ON OPTICAL QUALITIES OF A SPACECRAFT WINDOW

by David N. Warner, Jr., and Thomas M. Walsh

Ames Research Center
Moffett Field, Calif.

NATIONAL AERONAUTICS AND SPACE ADMINISTRATION • WASHINGTON, D. C. • OCTOBER 1968

TECH LIBRARY KAFB, NM
0131623

EFFECTS OF EDGE CONSTRAINTS ON OPTICAL QUALITIES OF A SPACECRAFT WINDOW

By David N. Warner, Jr., and Thomas M. Walsh

Ames Research Center
Moffett Field, Calif.

NATIONAL AERONAUTICS AND SPACE ADMINISTRATION

For sale by the Clearinghouse for Federal Scientific and Technical Information
Springfield, Virginia 22151 – CFSTI price $3.00

EFFECTS OF EDGE CONSTRAINTS ON OPTICAL QUALITIES OF A SPACECRAFT WINDOW

By David N. Warner, Jr., and Thomas M. Walsh

Ames Research Center

SUMMARY

Some effects of edge constraints on optical qualities of Gemini spacecraft windows were determined experimentally. Frames approaching theoretical fixed-edge and free-edge constraints were designed and constructed for the investigation. Gemini window frames were also used so that the idealized frames could be compared to an operational window frame.

Direct measurements were made of the flatness and wedge angle of the windowpanes, the resolution loss through the window, the angular deviation of a line of sight, and the distortion of a flat wave front traveling through the window assembly. Space pressure differentials were applied to the window to bow the panes and simulate the effect of the space environment.

Tests showed that edge constraints on spacecraft windows significantly affect their optical qualities. The qualities become more irregular, particularly at high incidence angles, as the panes are distorted in the simulated space environment. Although the clamped-edge frames did not provide a strictly theoretical fixed-edge condition, they did allow less surface deflection, less angular deviation to the line of sight, and less distortion to a plane wave front. The free-edge data, while similar to the clamped-edge data in uniformity, exhibited greater magnitudes of distortions and deviations. The Gemini frames caused greater, more irregular, wave-front distortions and angular deviations.

INTRODUCTION

Several optical experiments have been performed on the Gemini manned space flights, and others will be performed in the Apollo program. These experiments use the spacecraft windows as viewing ports; thus the windows are one component of the optical system. The surfaces of the windowpanes may be curved and nonparallel, and therefore may alter the direction of a line of sight through the window or distort a wave front being transmitted by the window. These effects are important to the results of experiments utilizing such instruments as sextants, pointing lasers, cameras, telescopes, and stadiometers.

The influence of edge constraints on the curvature and, in turn, on the optical qualities of a Gemini spacecraft window is the subject of this

experimental study. Only a limited number of studies have investigated the parameters that affect a window's optical characteristics. Reference 1 describes the experimentally measured characteristics of the left-hand, non-optical quality Gemini window. Reference 2 describes some measurements of sky luminance, spacecraft corona, scattered light, and glare sources for the Gemini windows. Reference 3 concerns studies of aircraft photographic windows.

Three types of frames with different edge conditions were used in this study. One was the Gemini spacecraft frames complete with actual gasketing and bolting. A second type was specially designed and constructed to provide a theoretical fixed-edge condition. The third type was a modification of these special frames to provide a theoretical free-edge condition. One set of three windowpanes was used; it was identical to Gemini model 133-P, high-optical quality windowpanes, except that they had no antireflection coatings. These panes are the type installed on the right-hand side of the Gemini spacecraft and used as a viewing port for optical experiments. Although the panes are of high optical quality, their bowing under space environment pressures causes significant angular deviation to a line of sight.

The window optical qualities determined as a function of edge constraint were: flatness of panes, degradation to resolution, deviation to a line of sight, and distortion to a plane wave front transmitted through the window. The wedge angle of each pane was determined. It was measured to note its uniformity over the window aperture because it directly affects the results that might otherwise be attributed to the flatness variation. The flatness of panes was measured before and after they were installed in the frames and again while bowed with environmental pressure. Under simulated space conditions, angular deviations of a line of sight were measured at various locations on the window, at various incidence angles, and in various planes. The distortion to a plane wave front passing through the window was measured interferometrically for various angles of incidence and various planes of incidence.

New techniques were developed for measuring flatness and angular deviation. When the windows are bowed by simulated space pressure, hundreds of interference rings are generated in the flatness interferometer, and these required a method of obtaining sufficient contrast for fringes over the large area of the panes. Specialized techniques and apparatus were also required for accumulating a great amount of deviation data without a zero shift greater than a second of arc during the test measurements.

WINDOW DESCRIPTION

Glass Configuration

The Gemini type, right-hand window being simulated in this study consisted of three panes of Corning Vycor 7913 fused silica. The allowable wedge angles, surface flatness, and resolution of each pane which are important to this study were as follows:

(1) The maximum wedge angle between the two glass surfaces of any pane cannot exceed 4 seconds of arc.

(2) Surface flatness over an area 6 inches in diameter in the approximate center of each pane must be within 2-1/2 wavelengths of sodium light and uniform within 1/8 wavelength.

(3) The panes cannot cause degradation of optical resolution exceeding 1-1/2 seconds of arc for the 35° incidence angle at which an astronaut looks out the window.

Tests of the windowpanes used in this study indicated they were equal to, or better than, the specifications outlined above.

The window shape (fig. 1) is approximately elliptical. The inner and center panes are identical in size, having a horizontal major axis of about 14 inches, and a vertical minor axis of about 8 inches. The outer pane is slightly larger, having a major axis of about 15-3/4 inches and a minor axis of about 8-1/2 inches. The inner and center panes are 0.380 inch thick, and the outer pane is 0.330 inch thick.

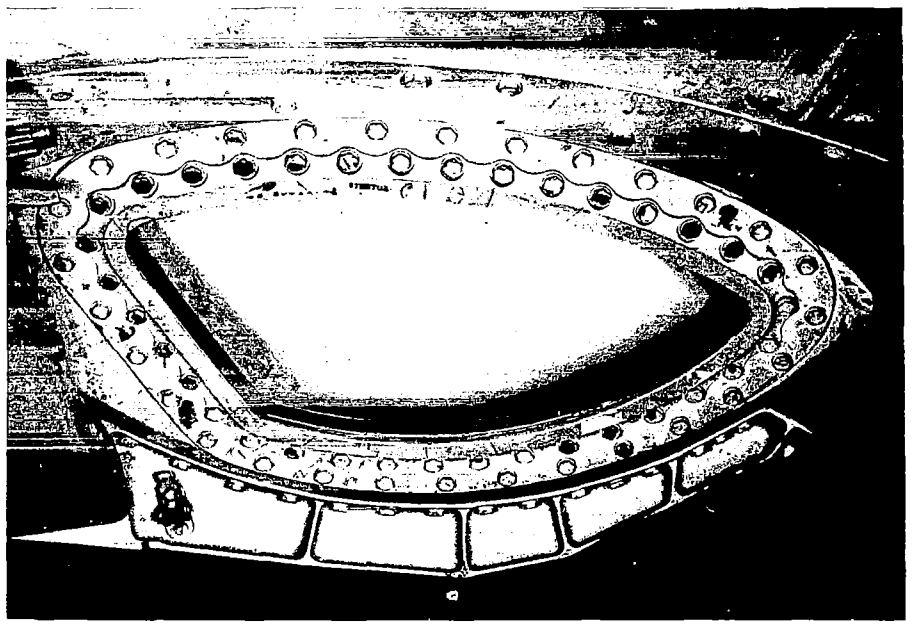

Figure 1.- Gemini window mounted in hatch.

Frame Construction

Gemini window configuration.- A cross section of the Gemini-type windo. frames used in this study is shown in figure 2. The inner and center panes are assembled as a unit with a titanium spacer between them. A 3/64-inch

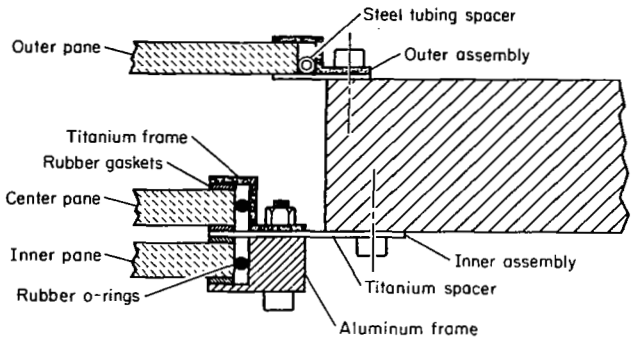

Figure 2.- Gemini-type frames.

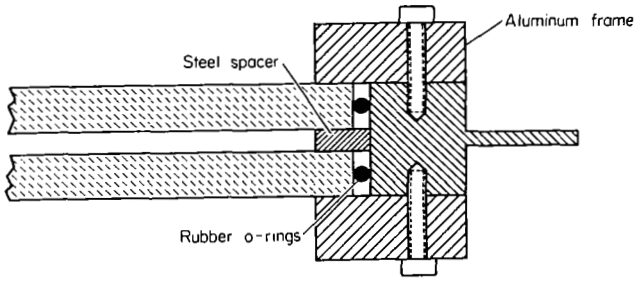

Figure 3.- Clamped-edge frames.

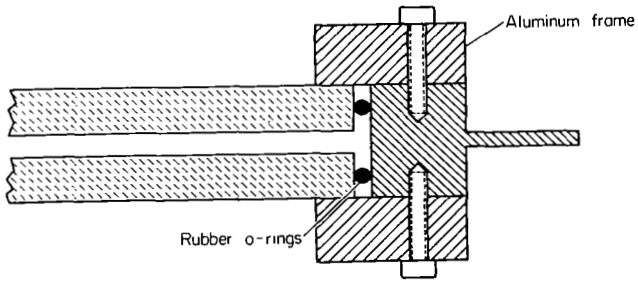

Figure 4.- Free-edge frames.

silicone rubber gasket is used on each side of each pane. A 35-inch-pound torque is used on the 35 frame bolts as the clamping force on the gaskets. This inner assembly serves as a pressure seal for the spacecraft interior which is at 5.5 psi. In actual use, the outer pane, which acts as a heat shield, is loosely held in a separate frame assembly mounted to the outer spacecraft skin. It is separated from the center pane by 1-1/4 inches and in space has a vacuum adjacent to both surfaces. The outer assembly was used without modification for this study, and the outer and inner assemblies were bolted to a 1-5/8-inch-thick aluminum plate.

Clamped-edge window configuration.- For the clamped-edge window simulation, the aluminum frame (fig. 3) was clamped against the outside surfaces of the glass panes. A solid steel spacer was clamped directly against the inside surfaces. No gaskets were used between these clamping surfaces, and 20 inch-pounds of torque was used on the 35 frame bolts to exert the clamping force.

Free-edge window configuration.- For the free-edge window, air pressure between the panes pressed the glass directly against the aluminum frames (fig. 4). There was no restriction (i.e., no gasket or metal spacer) between the inner surfaces. An O-ring seal was used around the outer edge of the panes to effect a pressure seal.

SIMULATION OF THE IN-FLIGHT WINDOW ENVIRONMENT

In order to obtain valid data on optical resolution degradation, line-of-sight deviations, and distortion to a transmitted wave front, the window must be tested in a real or simulated space environment. Of primary importance is

the pressure environment which causes a bowing of the windowpanes. In addition, the indices of refraction of the air surrounding the panes must correspond to those encountered in space. Since testing in the real space environment is not feasible, it was determined (ref. 1, appendix A) that increasing the air pressures uniformly 9.2 psi over those encountered in space flight, would provide a valid simulation of the space environment, as well as safe, convenient working conditions for the test crew. This resulted in the simulation pressures shown in figure 5. The window was mounted on one wall of a simulation chamber with the outer pane toward the inside. The chamber and the space between the outer and center pane were partially evacuated to 9.2 psi. The space between the center and inner pane was pressurized with air to 23.9 psi. Surface 1 of the inner pane was exposed to ambient laboratory pressure of 14.7 psi.

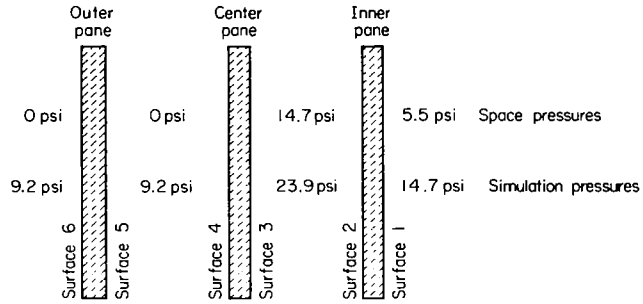

Figure 5.- Simulation pressures.

APPARATUS

Special optical equipment was necessary to obtain the interferometric and line of sight angular deviation data required for definitive study of the spacecraft window optical parameters. Because of the window's comparatively large size, commercially available autocollimators, interferometers, and related equipment would not perform the measurement tasks efficiently with the required precision of 1 second of arc. Therefore, a 12-inch-aperture optical system was developed that had a laser light source and 1/20 wavelength precision optical components as individual subsystems for obtaining the interference and deviation data. The components were designed for use in various appropriate arrangements on a granite surface plate. The inherent precision of the components and the soundness of the experimental design was demonstrated for a given test setup by the repeatability of data within a second of arc over intervals of several hours and by the agreement of data to within a second of arc when the setup was disassembled and reconstructed after several days.

Thin Film Interferometer

Surface flatness of each of the six unmounted glass surfaces was determined by the standard technique of interference comparison to a 7-inch-diameter optical reference flat (fig. 6). The reference surface was flat to within 1/20 wavelength of the 589 nanometers sodium light.

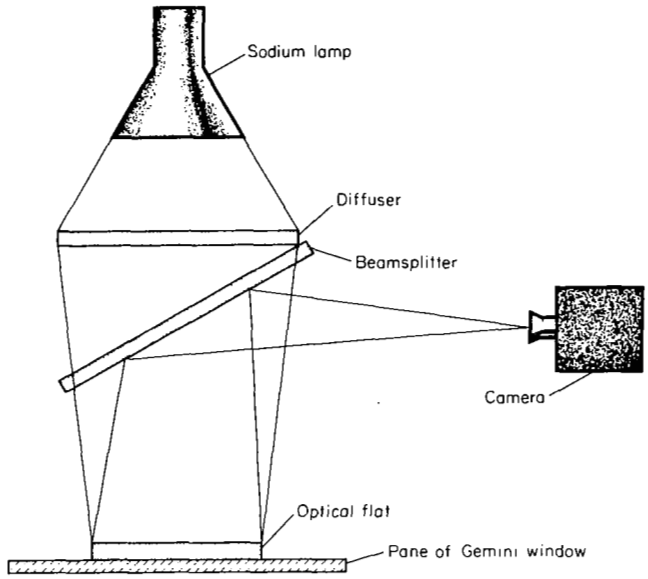

Figure 6.- Thin film interferometer.

Twyman-Green Interferometer

The optical components were arranged as a Twyman-Green interferometer for determining the flatness of the mounted windowpanes. The collimating lens had a 12-inch diameter and a 197-inch focal length, and the light source was a helium-neon gas laser of 632.8 nm wavelength (nominally 15 mW output power) with expanding lens and 0.002-inch aperture. (The light path was folded by means of two front surface mirrors to fit the system on the 6- by 12-foot granite surface plate.) To this basic lens-laser collimator, a 12-inch-diameter, 50-percent transmittance beamsplitter, and two 12-inch-diameter front surface mirrors were added to form the two arms of the interferometer (fig. 7). A camera with Polaroid type 55 PN film was used adjacent to the cube beamsplitter to record the interference patterns. The interferometer arms were adjusted to have approximately equal optical paths for maximum fringe contrast. To eliminate distracting diffraction patterns in the laser beam, a 25-micron aperture was used at the expanding lens focus. Alinement of the optical components was greatly simplified by temporarily removing the expanding lens and using the narrow laser beam as a visible indicator of the system axis. Individual components could then be easily and quickly alined on and normal to this axis. The interferometer produced fringe patterns accurate to 1/10 wavelength of 632.8 nm light over the 8- by 11-1/2-inch clear aperture.

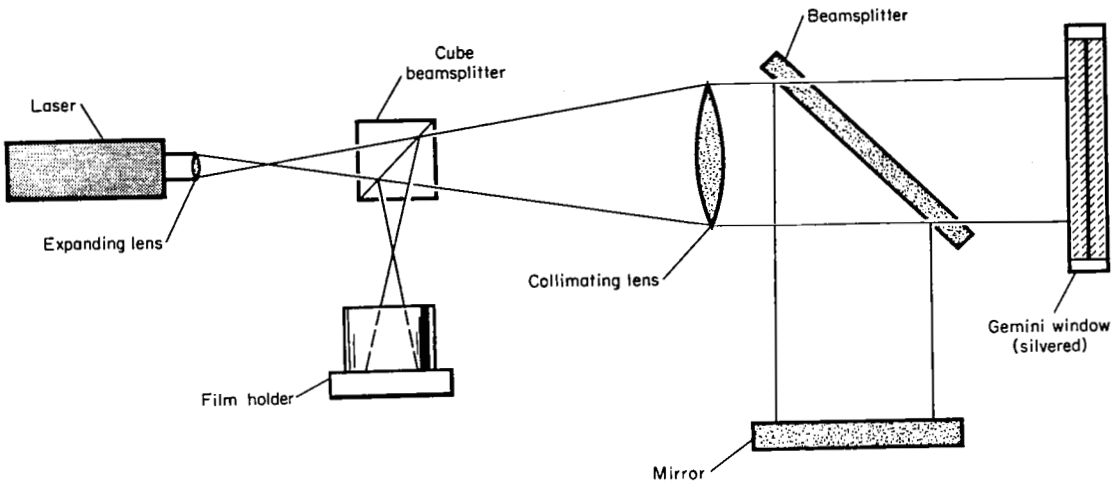

Figure 7.- Twyman-Green interferometer.

Wedge Interferometer

The wedge interferometer (fig. 8) used components that were described above. The collimating lens was large enough to provide an 11-1/2-inch-diameter bundle of highly collimated light. The windowpane provides its own reference in that the reflections at each surface interfere, yielding an interference pattern caused by the wedge or lack of parallelism between the surfaces.

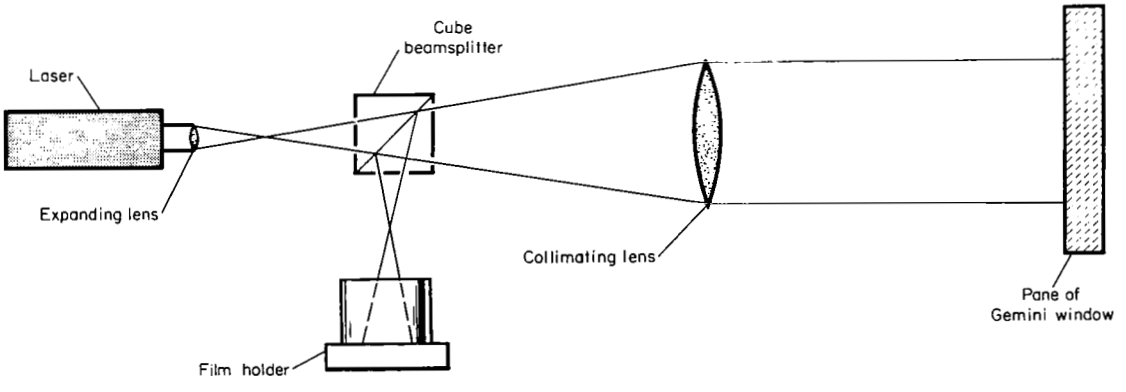

Figure 8.- Wedge interferometer.

Pressure Chamber

A special pressure chamber (fig. 11) was constructed to provide correct pressure differentials across the window. The window in its frames was bolted to a 1-5/8-inch-thick, 24-1/2-inch diameter aluminum plate clamped on the chamber front and pneumatically sealed with a thin rubber gasket. Orientation of the window was changed by rotating the aluminum mounting plate about its center. Incidence angles were changed by rotating the pressure chamber around an axis on window surface number 1. The granite surface plate acted as the chamber's bottom so that the 12-inch mirror inside the chamber would remain undisturbed when the chamber was moved. The air seal between chamber and surface plate was a 1/4-inch rubber O-ring. Precision regulators controlled the pressures inside the chamber and between the inner and center panes (fig. 5) to better than 0.1 psi.

Resolution Apparatus

The degradation of optical resolution caused by the window was measured with the apparatus shown in figure 9. A 6-inch mask limited the aperture so that no loss in aperture would be suffered as the window moved to a 35° incidence angle. The aperture was thus constant, and the only variable was angle of incidence. The rest of the equipment and the space environment pressures simulated by this equipment has been mentioned previously.

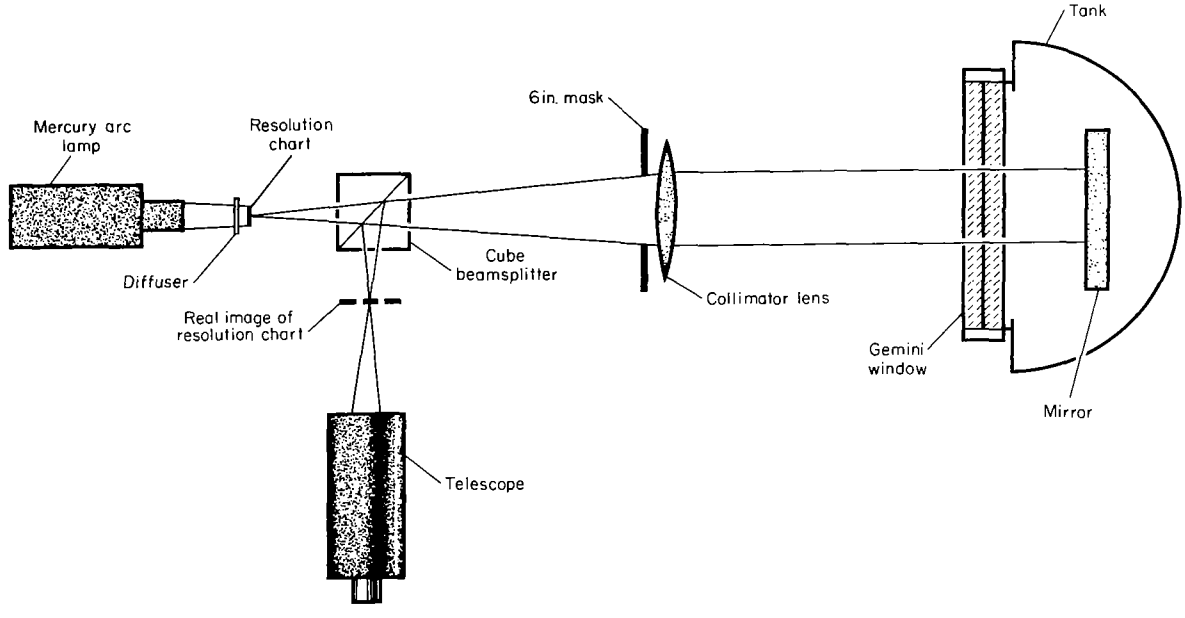

Figure 9.- Resolution test system.

Angular Deviation Test Apparatus

The optical components were arranged as shown in figures 10 and 11 as an autocollimator to measure window-induced line-of-sight deviations. The basic

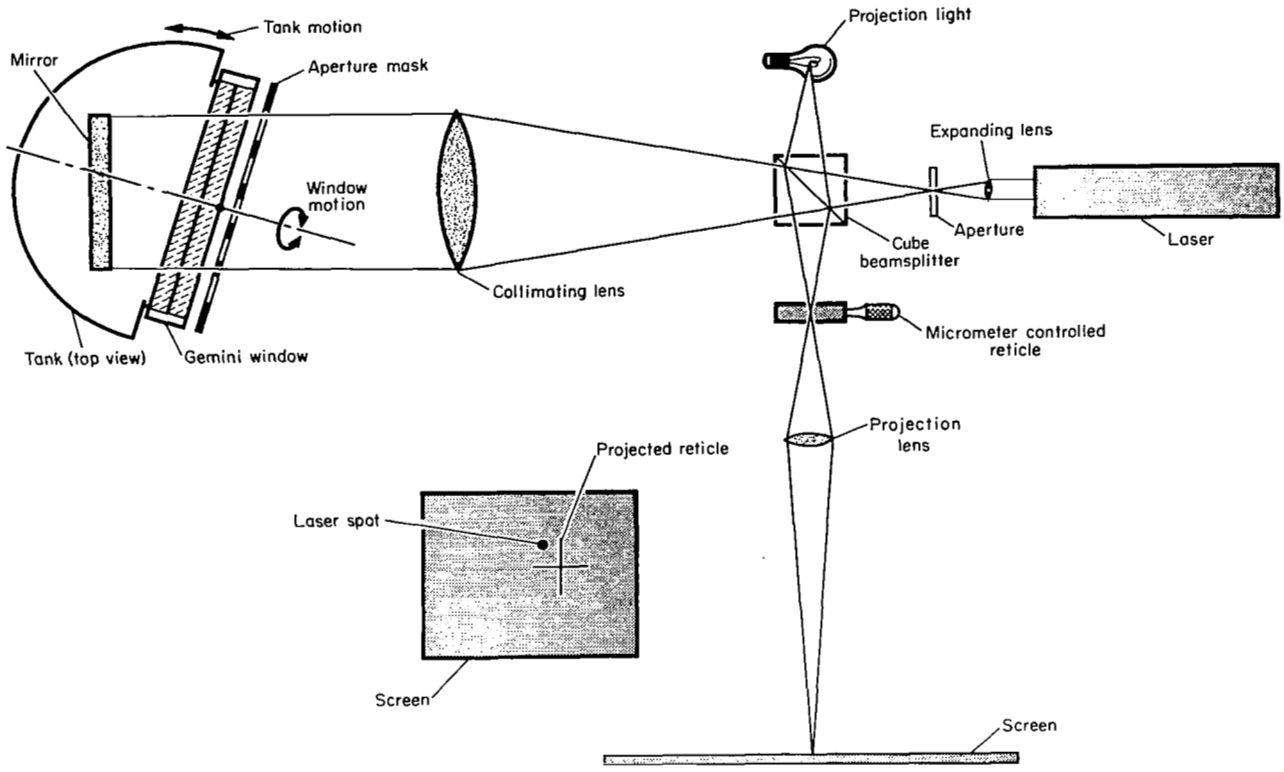

Figure 10.- Deviation measurement system.

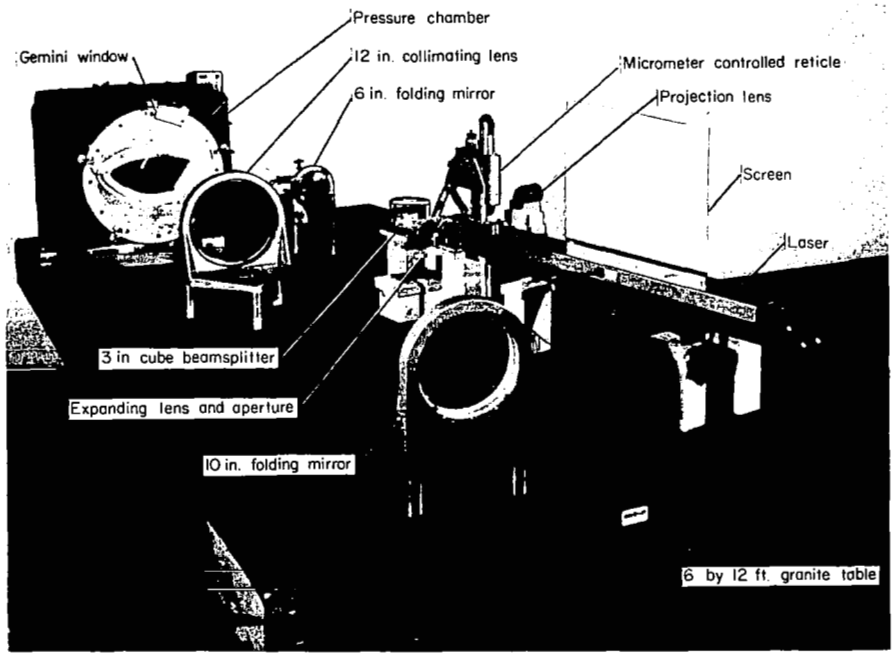

Figure 11.- Angular deviation test apparatus.

laser-lens collimator system produced a light bundle collimated to better than 1 second of arc in the central 8 inches. A 12-inch-diameter front surface mirror inside the pressure chamber reflected the collimated light back through the system to a 3-inch-cube beamsplitter. The light was then reflected to focus on a crosshair reticle mounted on a precision cross-slide adjustable in X-Y to 0.001 inch. For increased precision in adjusting the crosshair coincident with the focused light dot, the illuminated reticle and dot were projected on a screen at a magnification of approximately 30.

Transmitted Wave Interferometer

The transmitted wave interferograms were obtained by means of a Twyman-Green interferometer with the window installed in the test chamber as shown in figure 12. The equipment has been described previously under flatness measurement apparatus.

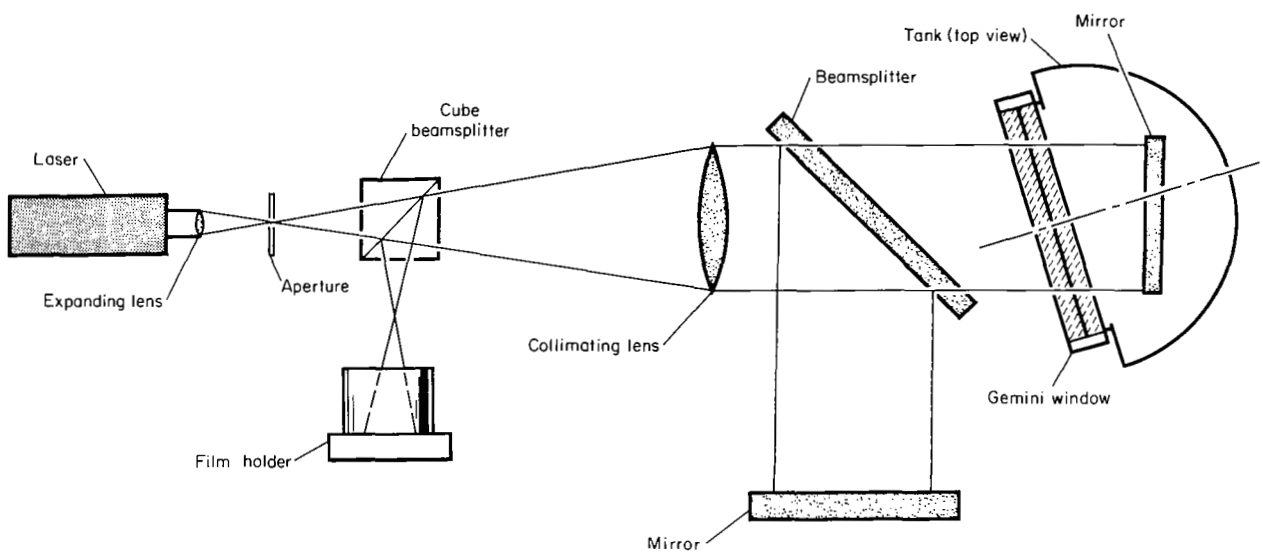

Figure 12.- Measuring transmitted wave with Twyman-Green interferometer.

PROCEDURES AND DATA ANALYSIS

Flatness Measurements - Unmounted Panes

The flatness of each of the six glass surfaces was determined by interference comparison to a 7-inch-diameter optical reference flat accurate to 1/20 wavelength. Sodium light was used. These tests were made before the windowpanes were mounted in their frames. The low thickness-to-width ratio of the panes (about 1/50) led to concern as to how much the panes would deflect if ordinary test procedures were used. First, a pane was laid directly on a micro-flat granite surface plate of comparable flatness to the pane. The 7-inch reference flat was held above the pane by a special trident

support so no weight of the reference flat was transmitted to the pane. A flatness interferogram was then obtained from interference between the pane and the reference flat. The pane was then rotated in azimuth on the granite surface plate and another interferogram obtained. Changes in flatness of the order of only 1/2 fringe were observed. (If the pane deflected to the contour of the granite surface plate the interferogram would have changed by four fringes.) Secondly, an aluminum plate covered with velvet was interposed between the granite plate and the windowpane. The change with window orientation in azimuth on the velvet-covered plate was of the order of 1/2 fringe. Thirdly, the full weight of the 7-inch reference flat was lowered onto the pane, first with the pane directly on the granite surface plate, and then with the velvet-covered plate interposed. The weight of the reference flat changed the flatness of the pane by the order of about one fringe in each case. Flatness of the pane thus is the same, to the order of at least one fringe, when supported by any of these methods. The procedure adopted to obtain the flatness of the thin panes was to place the windowpane on the velvet-covered plate and the reference flat directly on the pane so as to obtain high contrast fringes.

Flatness was measured with the thin film interferometer without any particular orientation of the reference flat relative to the windowpane other than nominally parallel. The axes of the source and of the viewing point were roughly over the center and normal to the reference flat as shown in figure 6. The interferometer under these conditions gave equal thickness fringes of the air wedge between the window and the reference surface. The straightness of these fringes indicates the flatness of the windowpane surface. A deviation of one fringe spacing (dark to dark) from a straight line is equivalent to 1/2-wavelength deviation of the window surface from a flat plane. Since the reference surface is flat to 1/20 wavelength, the interferogram can be read by interpolation of the fringe spacing to 1/20 wavelength.

Flatness information was also deduced from wedge photographs. Curvature of the fringes indicates deviation from flat normal to the direction of wedge. Irregular spacing of the wedge fringes indicates deviation from flat in the direction of wedge. The deviation from flat could be due to either or both surfaces. Flatness measurements obtained from the wedge photographs compared well with the reference flat measurements.

Flatness Measurements - Mounted Panes

Measuring the flatness of the windowpanes as mounted in their frames in the simulated space environment and with proper pressures applied constituted a special problem. The deflection of the glass was so great that over 500 fringes had to be resolved on the film of the interferograms. A mirror reference surface had to be used with silvered windowpanes in the Twyman-Green interferometer system (fig. 7) in order to get sufficient contrast to record all the fringes on film. A process was developed for silvering the surface of the panes without altering the flatness to a fraction of a wavelength of light, and the silver was applied and removed as required during the course of this study. For testing in the mounted configuration,

surfaces 1 and 4 were silvered and placed in one arm of the Twyman-Green interferometer which was illuminated by a helium-neon gas laser of 632.8 nm wavelength (fig. 7). Flatness interference patterns of two external surfaces (numbers 1 and 4, fig. 5) were photographed to determine the effects of mounting and of applying the proper simulation pressures between the panes. Measurements were made on the photographs to determine the number and spacing of the interference fringes when simulation pressures were applied. Surface distortion versus fringe spacing along the vertical axis of the window was determined and plotted.

For the flatness measurements with the Twyman-Green interferometer, the reference mirror was oriented parallel to the mean plane of the windowpane when unbowed by pressure. The orientation of the reference mirror was not changed when bowing pressures were applied to the window. With a 1/20 wavelength quality mirror substituted for the window, the interferometer checked to 1/10 wavelength quality as a system. A fringe deviating from a straight line by one fringe spacing represents a 1/2 wavelength deviation of the windowpane from a flat pane at that fringe location. Interference fringes were counted downward from the high point along the vertical center line of the window. One fringe space is equal to 1/2 wavelength of light, or 632.8 nm, which is 12.4×10^{-6} inch. The coordinate locations of the high point and of the fringes were measured relative to the reference axes of the window by scaling the photographs. The location of this apparent high point is determined by the orientation of the reference flat surface relative to the window. In these tests, the reference flat was adjusted parallel to the window to within ±16 seconds of arc before simulation pressures were applied to the window. Because of probable deflection of the frames at the edges under bowing pressures, and also because of the lack of exact parallelism in adjustment of the reference flat relative to the window, the top and bottom edges of the window do not plot as equal deflections down from the high point. The inequality is slight, however. Theoretical curves were computed as in reference 4 for the top and bottom edges in the same plane.

Wedge-Angle-Measurements

The maximum wedge angle of each pane was determined with the wedge interferometer of figure 8. Reflections from each surface of the window, resulting from amplitude division of the incident light, produce equal thickness Fizeau fringes which were photographed. The fringe spacings on these photographs were measured to determine wedge angles in the direction of maximum wedge by means of the relation $\phi = N\lambda/2Ln$ where

ϕ wedge angle in radians

N number of fringes in zone

λ wavelength of light in air, in.

L length of zone, in.

n index of refraction

The formula $\phi = 2.57N/Ln$ gives the wedge angle in seconds of arc.

The precision of the wedge interferometer system is 1/10 wavelength which is equivalent to 1/5 fringe space. There were approximately 10 fringes in the 11-1/2-inch zone so the wedge was 1.5 seconds of arc. For this case, a 1/5 fringe error in fringe spacing is equal to less than 0.01 second wedge error. A 1/32-inch error in measurement of fringe zone length, added to a 1/8-inch error in either photographic distortion or scaling of the photograph, results in 0.02 second wedge error. Thus, the procedure should provide wedge measurements with errors of less than 0.1 second of arc.

Resolution Measurements

The effects of the optical quality Gemini window on resolution of an optical system were determined by observing a USAF 1X resolution test chart through the window mounted in the Gemini-type frames (fig. 9). The test chart was placed at the focal point of the collimating lens so that collimated light passed through the window. The 197-inch focal length collimator lens was masked to a 6-inch aperture and the smallest chart line spacing corresponded to an angular resolution of less than 1 second of arc. The pressure tank was used to simulate space pressure environment. The procedure (illustrated in fig. 9) of having a double transmission through the window resulted in more degradation than for the actual single transmission. To estimate the line pairs resolved, the real image was observed visually with a telescope. Photographic records were also made and the minimum line spacing resolved was converted to angular resolution. It became obvious that the degradation to resolution due to the window was minor and approached the resolution limit of the system. The resolution of the unmounted windows was similar to that of the windows in the Gemini-type frames so the contribution of the frame was negligible. Therefore, resolution tests for the clamped and free frames were omitted.

Resolution measurements were subjective; the concensus of three observers was used for each test condition. A resolution evaluation was made of the system of figure 9 without the window in the system, and the system was good to the Raleigh limit of the 6-inch aperture of the system, or about 0.8 second of arc.

Line-of-Sight-Deviation Measurements

The angular deviations of several lines of sight through the window were measured with the 12-inch aperture autocollimator (fig. 10). A mask with 1-inch-diameter apertures, which could be opened individually, was used to cover the window. Measurements were made for apertures A-4, C-2, C-4, C-6,

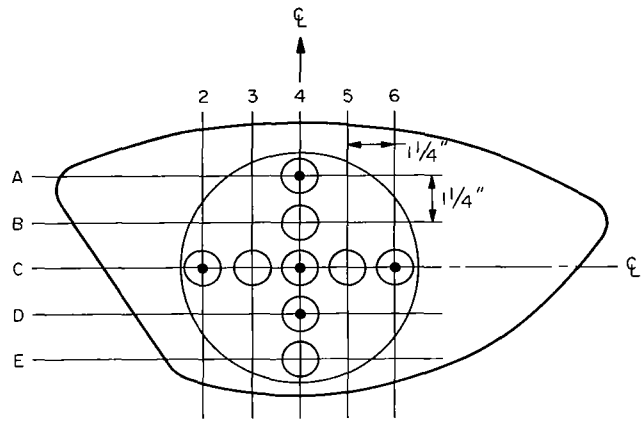

Figure 13.- Aperture spacing.

and D-4 (fig. 13), with incidence angles of 0°, 15°, 30°, and 45°, and orientation angles (fig. 14) of 0°, 45°, 90°, 135°, and 180°. Deviations were measured for the three frame conditions at the simulation pressures described previously. The deviations were measured in two components, one in the plane of incidence and the other perpendicular to that plane. The component in the plane of incidence includes refraction due to refractive index differences of the air on either side of the window, as well as refraction due to properties of the glass. Refraction due to the air is dependent on incidence angle, and is -6, -12, and -21 seconds of arc for incidence angles of 15°, 30°, and 45°, respectively, for the air densities involved (ref. 1). These values of refraction were subtracted from the data to determine how the error contributed by the glass alone was affected by frame constraint conditions.

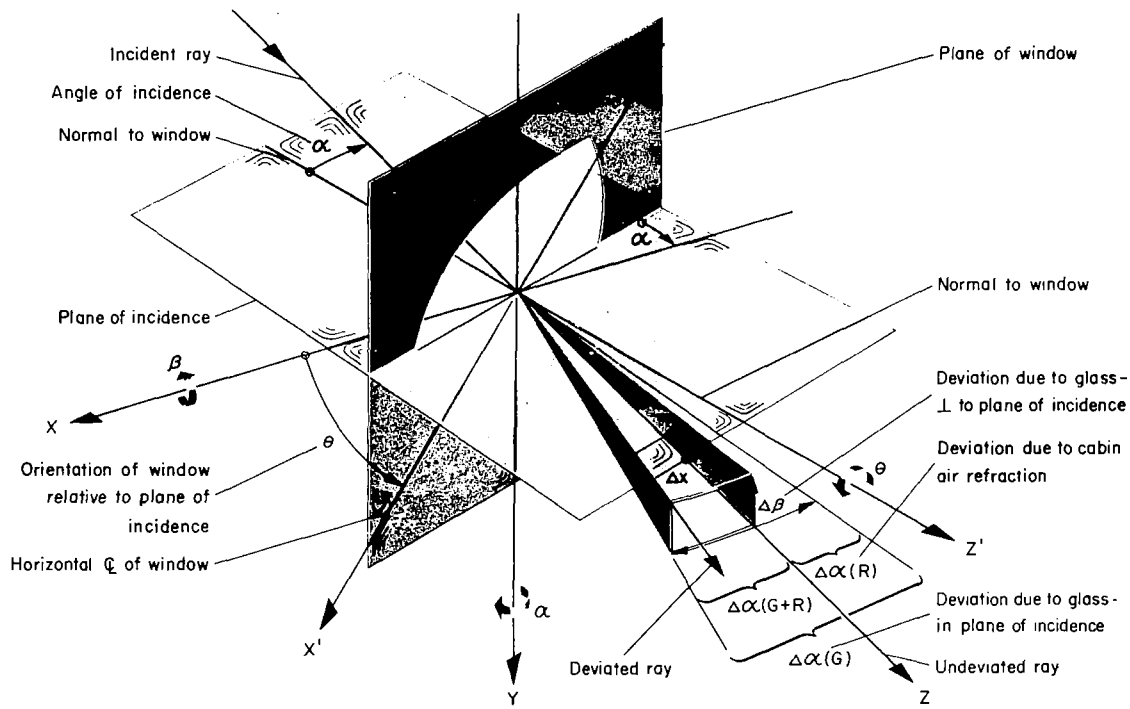

Figure 14.- Orientation of window-induced deviation errors.

The precision of the deviation measurements depends mainly on the focal length of the collimating lens. Thus,

$$\Delta\beta = \frac{\Delta Y}{2 \times \text{F.L.} \times 4.848 \times 10^{-6}} = 0.523\Delta Y$$

$$\Delta\alpha(G + R) = \Delta\alpha(R) + \Delta\alpha(G)$$

and

$$\Delta\alpha(G + R) = \Delta\alpha(R) + 0.523\Delta X$$

where the values and signs are as indicated in figure 14, and ΔX and ΔY, the cross-slide motions, are in inches. For a cross-slide motion of 0.001 inch, the deviation angle change is 0.523 second of arc. The least count of the cross slide is 0.001 inch, but the error of the operator setting of the cross-hair on the focused laser spot has a 1σ (standard deviation) of 0.0005 inch. As mentioned previously, the reference bundle of light through the window was collimated to within 1 second of arc. Thus, the maximum measurement error was limited to the collimation achieved in the reference bundle. Calibration wedges of glass certified to 0.1 second of arc were inserted into the system in lieu of the window to verify the precision of readout and to verify the direction of deviation.

Transmitted Wave Measurements

The Twyman-Green interferometer (fig. 12) was used to determine the distortion of a plane wave front passing through the window. The interferometer was initially adjusted so that no fringes were visible over its aperture. The fringe patterns were photographed as the window, mounted in the simulator chamber, was introduced into an arm of the interferometer and moved to incidence angles of 0°, 15°, 30°, and 45° at the 90° orientation angle (fig. 14). Photographs were made before and after simulation pressures were applied to the window mounted in the various frames. An elliptical area about 8 by 11-1/2 inches was examined for each test case. The photographs showed the regularity across the window and indicated the changes that occurred for the different frame types when the pressures were applied.

The transmitted wave interferograms have the same 1/10 wavelength precision as the flatness measurements discussed previously, since the same interferometer was used. The reference (plane) wave front was flat to 1/10 wavelength by measurement in the central 8 inches of diameter. Before the window was inserted, the two reference mirrors were alined to be parallel so that no fringes were observed in the 12-inch aperture. The transmitted wave fringes that are seen with the window inserted represent the changes to a flat wave front. Each fringe spacing represents an elevation change of 12.4×10^{-6} inch, and to the same scale, the variation of a fringe from a straight line indicates the curvature of the wave front.

RESULTS

Flatness of Unmounted Panes

The surface flatness of each of the three unmounted Gemini windowpanes was determined with the thin film interferometer previously described. The surfaces of the unmounted panes are basically spherical as indicated by the smooth circular curvature of the fringes in figure 15. The small circles denote aperture locations 1-1/4 inches on center. Deviation of the surfaces from a flat plane was only 1-1/2 to 2-3/4 wavelengths, as seen in the table below. For glass of this small thickness-to-width ratio (about 1/50), this flatness constitutes high optical quality.

Flatness Test Results of Unmounted Panes

Surface	Maximum flatness deviation from 7-inch flat (wavelengths at 589 nm)
1	1-1/2 convex
2	1-1/2 concave
3	1-1/2 convex
4	2 concave
5	2 convex
6	3 concave

Flatness of Panes Mounted in Frames

Gemini-type frames.- Mounting the panes in the Gemini-type frames without bowing pressure distorted the surfaces into complex shapes. Surfaces 1, 4, 5, and 6 became compound surfaces, that is, convex along one cross section and concave along another (fig. 16). They deviated as much as 69 wavelengths from a plane (see table following). When simulation pressures were applied, surfaces 1 and 4 distorted into high curvature ellipsoidal surfaces as evidenced by the eccentric bulls-eye pattern in figures 16(b) and (d).

Clamped-edge frames.- The clamped-edge frames distorted the panes less than the Gemini-type frames. Surface 4 was distorted about half as much as in the Gemini-type frames when pressurized, as shown in the table following.

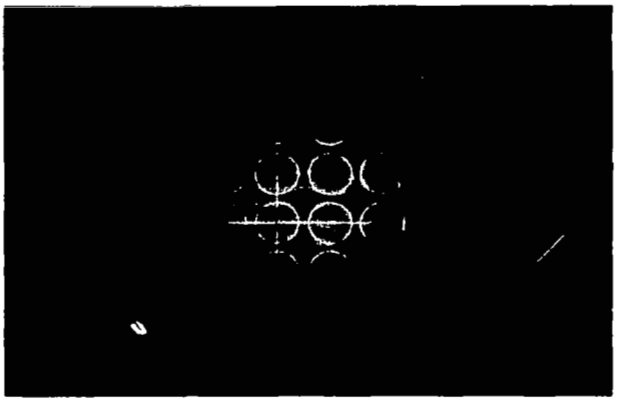

(a) Surface 1

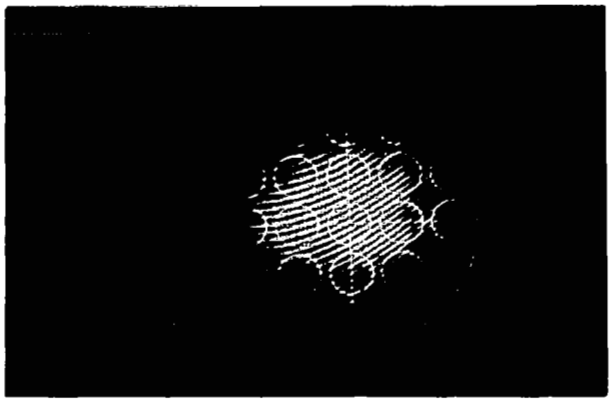

(b) Surface 4

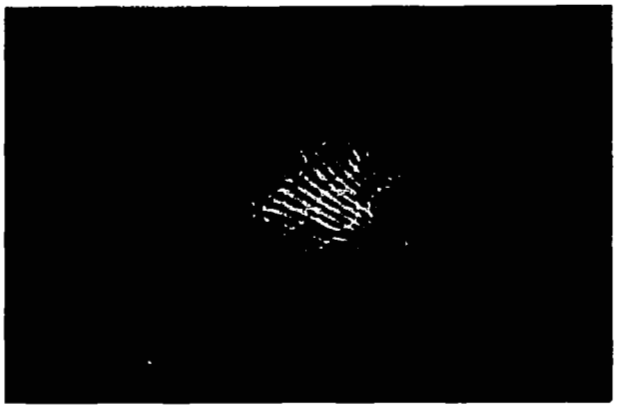

(c) Surface 5

(d) Surface 6

Figure 15.- Flatness interferograms of unmounted panes.

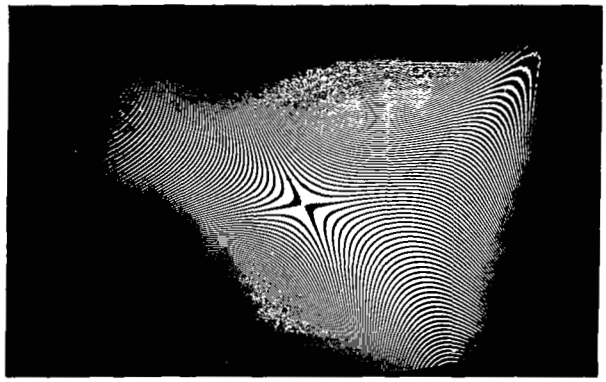

(a) Surface 1 with no pressure.

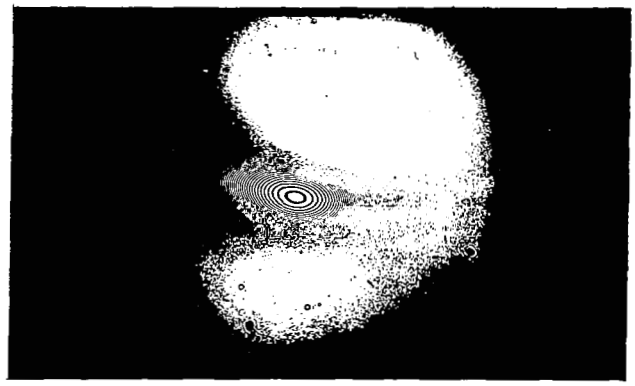

(b) Surface 1 with simulation pressures.

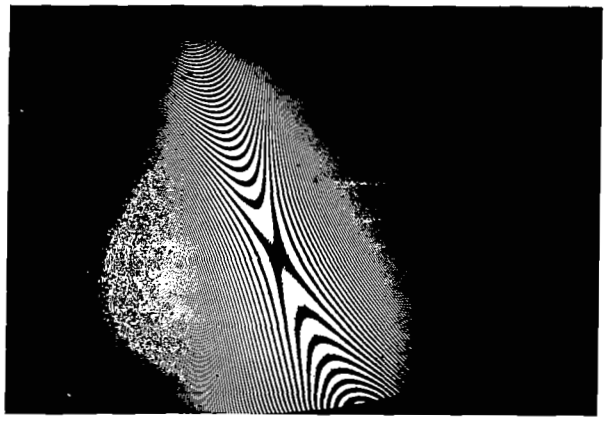

(c) Surface 4 with no pressure.

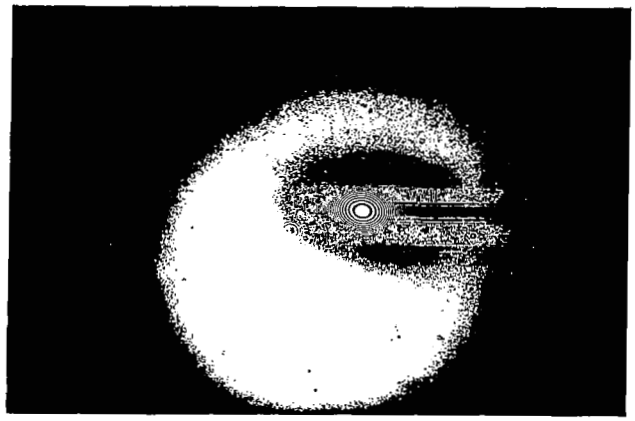

(d) Surface 4 with simulation pressures.

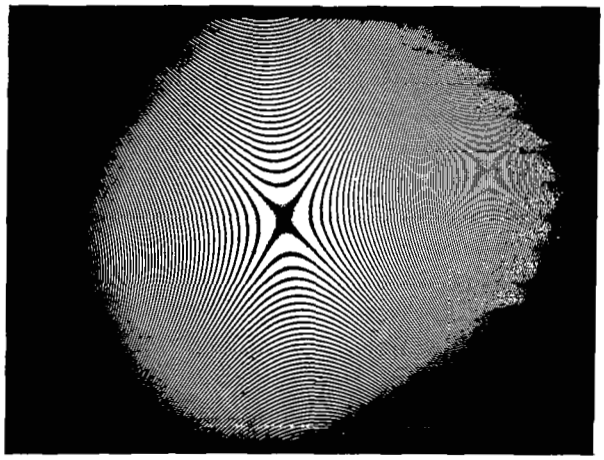

(e) Surface 5 with no pressure.

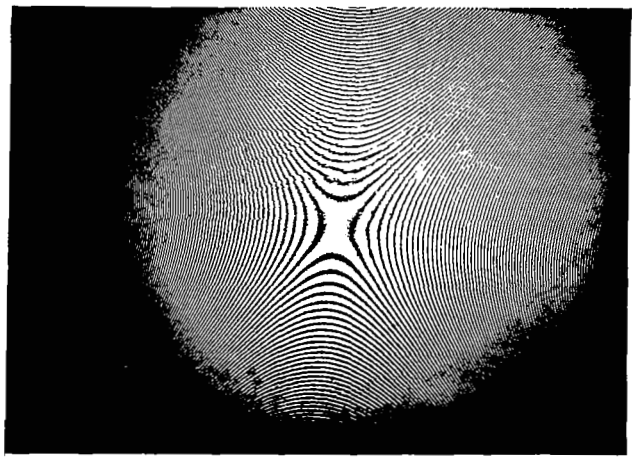

(f) Surface 6 with no pressure.

Figure 16.- Flatness interferograms of panes mounted in Gemini frames.

Flatness Test Results for Mounted Panes

Surface	Maximum flatness deviation (wavelengths at 632.8 nm)	
	No pressure	Pressurized
	Gemini	
1	16 convex, 39 concave	185 convex
4	69 convex, 10 concave	248 convex
5	18 convex, 30 concave	--
6	26 convex, 19 concave	--
	Clamped Edge	
1	9 convex, 15 concave	91 convex
4	22 convex, 9 concave	132 convex
	Free Edge	
1	5 convex	163 convex
4	7 concave	245 convex

Localized clamping action at the edges of the window is apparent in the interferograms of figures 17(a) and (c). As with the Gemini-type frame the distortion pattern under pressure is a high curvature convex surface with all trace of the characteristics of the unpressurized patterns lost.

Free-edge frames.- The free-edge frames caused much less distortion than the Gemini-type frames, as seen from the table following and the interferograms of figures 18(a) and (c). The compound surface did not appear, and a distorted spherical surface has appeared with only seven wavelengths deviation from flat on surface 4. When pressure was applied, surfaces 1 and 4 exhibited high curvature similar to the surfaces in the Gemini-type frame.

The preceding flatness interferograms can be analyzed in more detail to determine the flatness along the vertical center line for each edge constraint. A comparison of the flatness along this line with the theoretical free- and fixed-edge constraints yields additional information on the behavior of these thin windows as a function of edge constraint. This

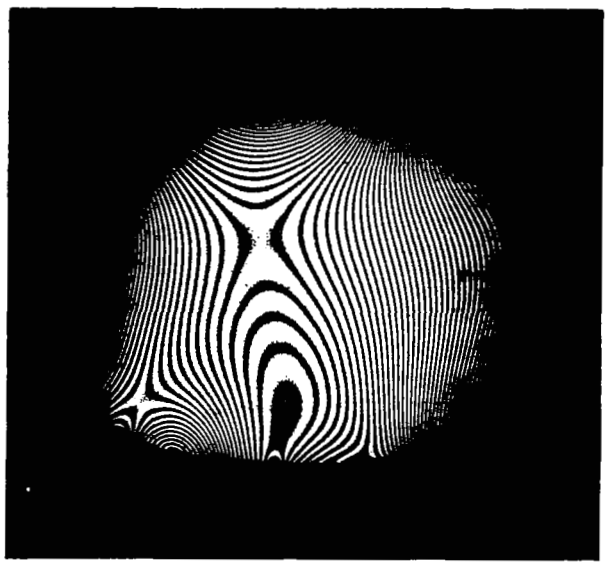

(a) Surface 1 with no pressure.

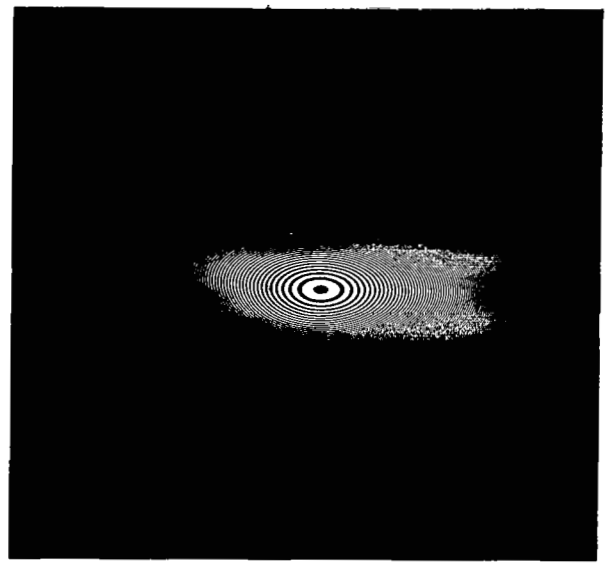

(b) Surface 1 with simulation pressures.

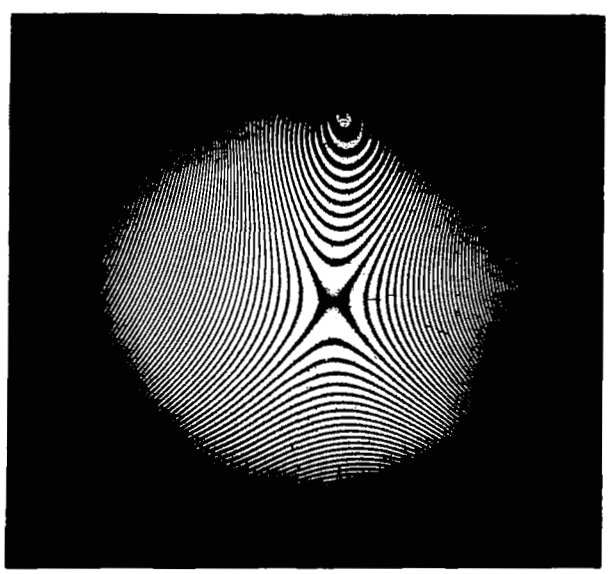

(c) Surface 4 with no pressure.

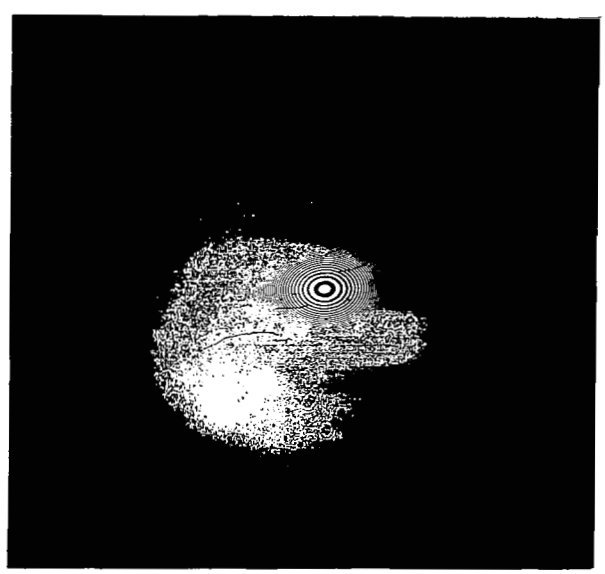

(d) Surface 4 with simulation pressures.

Figure 17.- Flatness interferograms using clamped-edge frames.

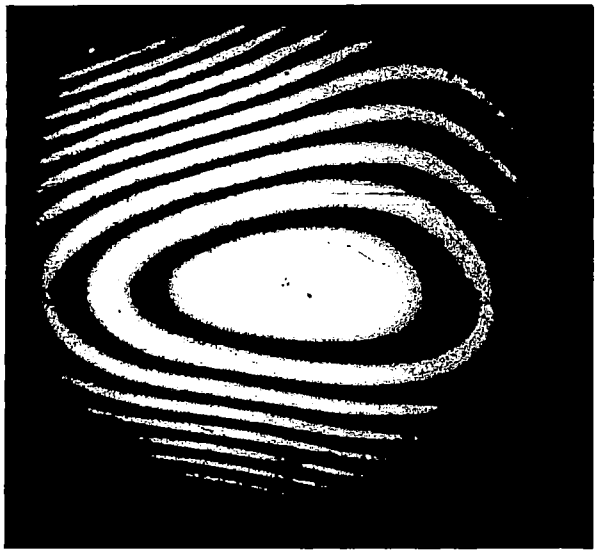

(a) Surface 1 with no pressure.

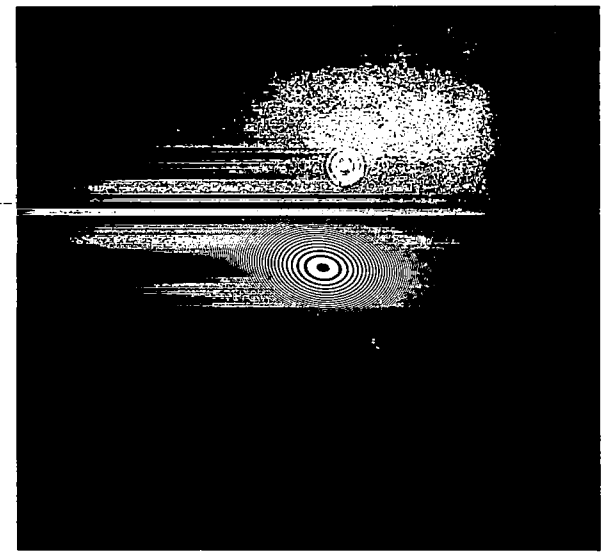

(b) Surface 1 with simulation pressures.

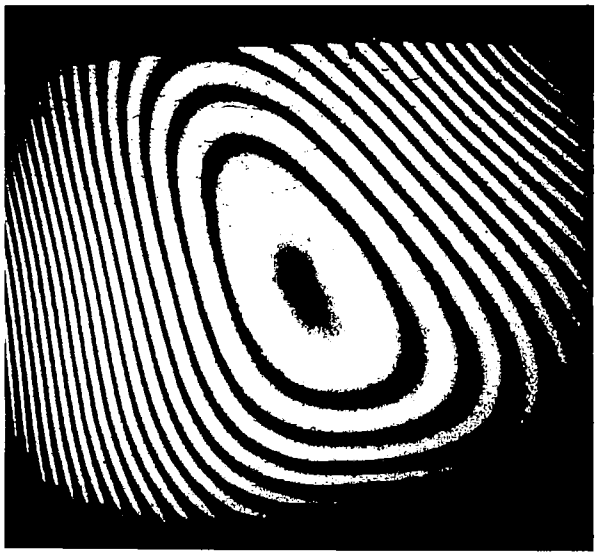

(c) Surface 4 with no pressure.

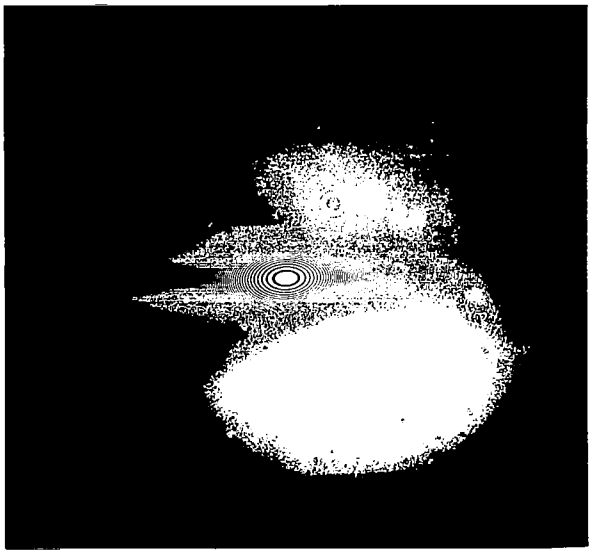

(d) Surface 4 with simulation pressures.

Figure 18.- Flatness interferograms using free-edge frames.

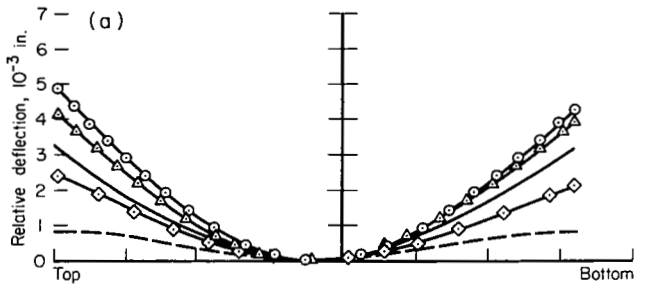

(a) Surface 1; 9.2 psi differential.

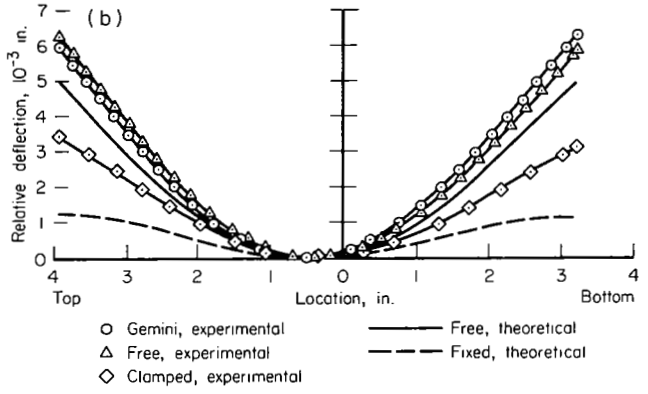

(b) Surface 1; 14.7 psi differential.

Figure 19.- Deflection of panes along vertical axis with pressure.

flatness information is plotted in figure 19 as surface deflection versus vertical location. It can be seen first that the curves for the Gemini-type and free-edge experimental frames are similar. Secondly, the experimental clamped-edge constraint did not closely approach a fixed-edge constraint. It is evident that zero slope at the extreme edge, as shown by the theoretical curve, could not be maintained. It is clear that the theoretical fixed edge yields less deflection than the others, and that the clamped edge yields less deflection than the other experimental edge constraints, and was consistent in that sense. A third bit of information revealed by figure 19 is that both the Gemini-type and experimental free-edge constraints permitted more deflection than the theoretical free edge. The disparity is not great, but it does indicate that the frame allowed or caused the glass to deflect more than a theoretical free edge. Any displacement of the test frame edges could release more glass to pressure bowing or any rotation of the frame could add torque to the glass edges to cause more deflection. A more rigid frame would exhibit less difference from the theoretical free edge, so it is apparent that the Gemini frame is less stiff than the free-edge experimental frame. The difference in deflection of the top and bottom of the panes, as seen in figure 19, is partly due to lack of parallelism of the reference surface and partly to movement of the top of the frame relative to the bottom.

Wedge-Angle Measurements

The wedge angle of the three panes of glass, as measured by the wedge interferometer, varied from 1 to 3 seconds of arc across the aperture observed. The aperture included the full height of the window at the vertical center line. The average wedge angle in the direction of maximum wedge was about 2 seconds of arc in each pane, as shown in the table. The panes were generally lens-shaped with the thick section at the top of the interferograms, as seen in figure 20.

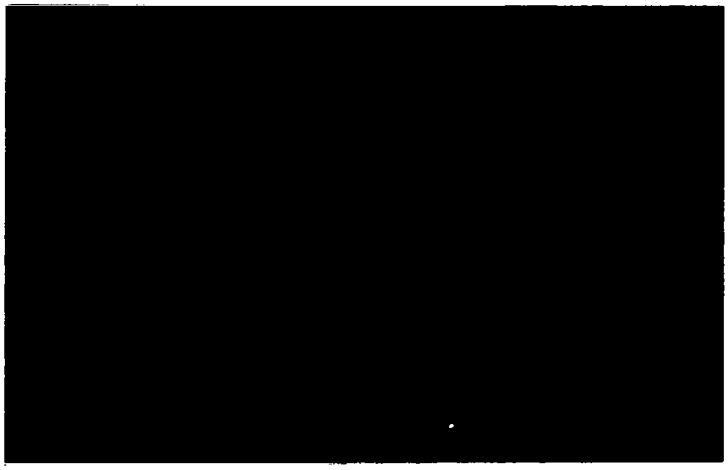

(a) Inner pane.

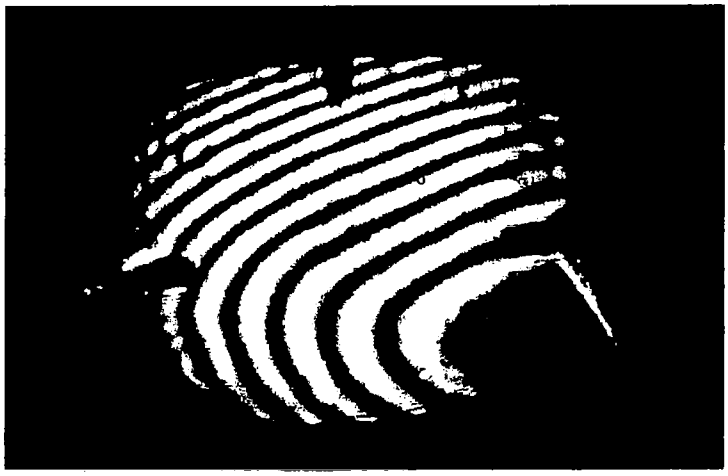

(b) Center pane.

(c) Outer pane.

Figure 20.- Wedge interferograms.

Wedge-Angle Test Results

Pane	Average wedge angle (arc sec)
Inner	2.1
Center	2.3
Outer	2.2

Resolution Measurements

Resolution was measured in the test setup shown in figure 9, according to the test procedures previously discussed. The tests show that resolution is somewhat degraded by mounting the window in Gemini-type frames, as can be seen in figure 21. These data indicate that angular resolution was degraded to about 3 seconds of arc at 35° incidence angle when simulation pressure was applied to the window. Refocusing the observing telescope when incidence was changed did not improve resolution, showing that the window does not tend to converge or diverge the light in a regular manner. It should be noted that the double pass through the window should cause more degradation than would be anticipated by a single pass. The window is apparently capable of accommodating the resolution limit of an optical system of about a 2-inch aperture which is about 2.5 seconds of arc.

Line-of-Sight Deviations

The effect of edge constraints on the angular deviations of several lines of sight through the window was measured with the test system of figure 9. The deviations are shown in figures 22, 23, 24, and 25, as a function of orientation angle for two apertures at two different incidence angles for each of three edge constraints. It can be seen from figures 22 and 24 that all the deviations for both apertures, C-2 and C-4, at 15° incidence, both in the plane of incidence and normal to it, and for all edge constraints, are less than 8 seconds of arc. This is true also for all the data listed in table I for 15° incidence which includes three additional apertures. The maximum spread between the deviations as a function of edge constraint is half of this, or 4 seconds of arc for the 15° incidence. Thus, there is only a slight effect of edge constraint of the windows on angular deviation at 15° incidence.

The angular deviations for 45° incidence for C-4 (fig. 25), the central aperture, show a cyclic variation of amplitude as a function of plane of incidence. The effect of edge constraint seems to be a fairly uniform step change in magnitude in the plane of incidence without affecting the cyclic pattern. The central aperture thus was little affected by type of edge constraint. Figure 23 shows the more typical variation of deviations, in the case for aperture C-2, which is 2-1/2 inches to the left of center on the horizontal center line. The Gemini-type frame caused large deviations coupled with wide variations as a function of plane of incidence. The free edge and

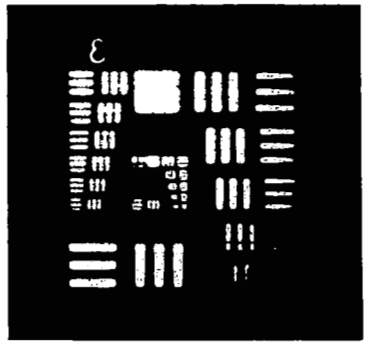

Resolution
0.7 sec

(a) Collimator with no window.

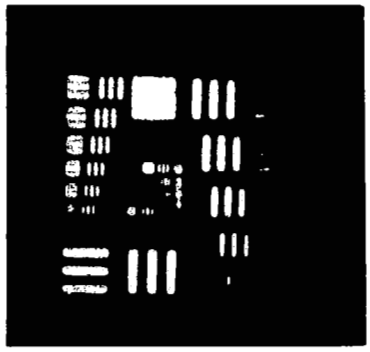

Resolution
1.1 sec

(b) Window normal to collimator axis with no pressure.

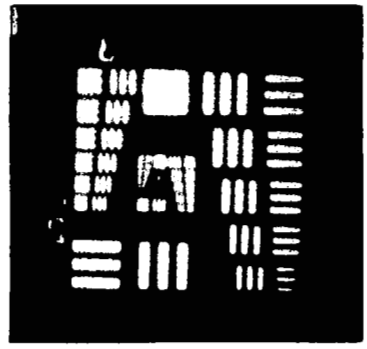

Resolution
1.0 sec

(c) Window normal with simulation pressures.

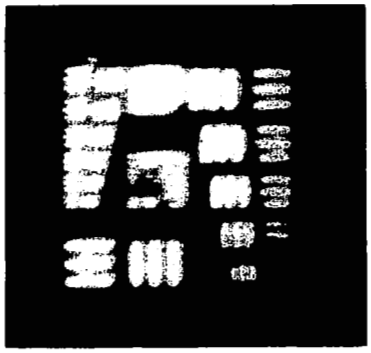

Resolution
1.4 sec

(d) Window at 35° with no pressure.

Resolution
2.9 sec

(e) Window at 35° with simulation pressures.

Figure 21.- Resolution test photographs with Gemini-type frames.

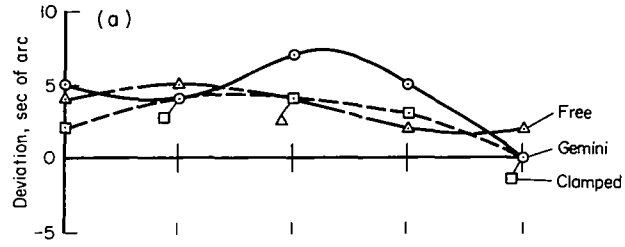

(a) Deviation in plane of incidence due to glass subjected to simulation pressure.

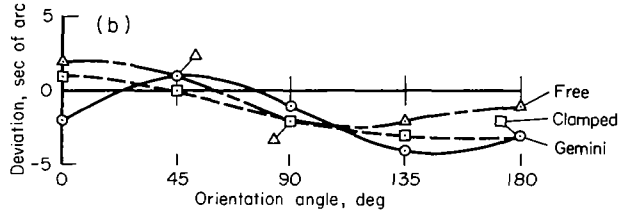

(b) Deviation perpendicular to plane of incidence due to glass subjected to simulation pressure.

Figure 22.- Line-of-sight deviations, aperture C-2, 15° incidence.

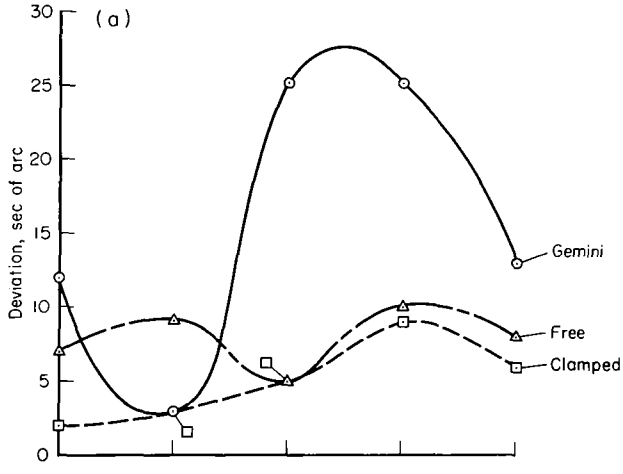

(a) Deviation in plane of incidence due to glass subjected to simulation pressure.

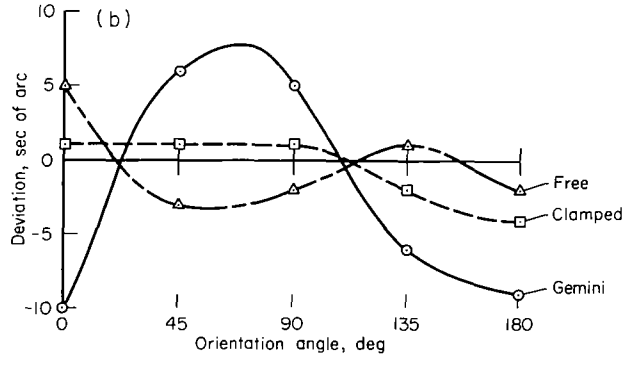

(b) Deviation perpendicular to plane of incidence due to glass subjected to simulation pressure.

Figure 23.- Line-of-sight deviations, aperture C-2, 45° incidence.

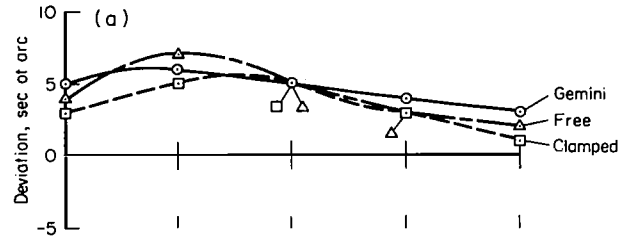

(a) Deviation in plane of incidence due to glass subjected to simulation pressure.

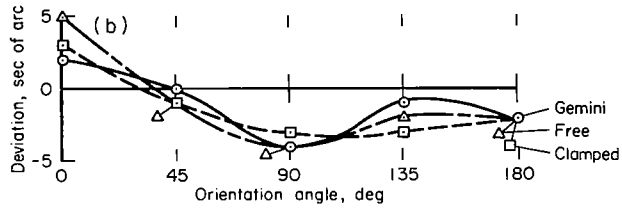

(b) Deviation perpendicular to plane of incidence due to glass subjected to simulation pressure.

Figure 24.- Line-of-sight deviations, aperture C-4, 15° incidence.

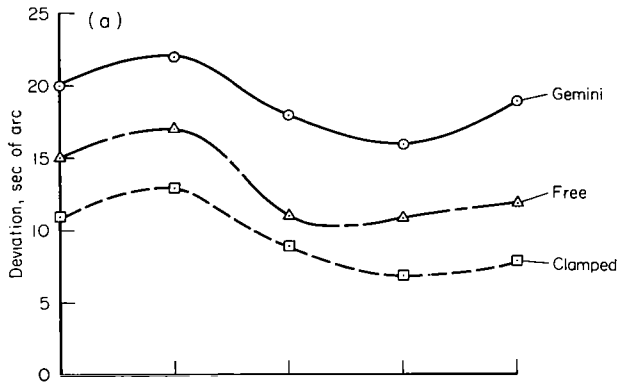

(a) Deviation in plane of incidence due to glass subjected to simulation pressure.

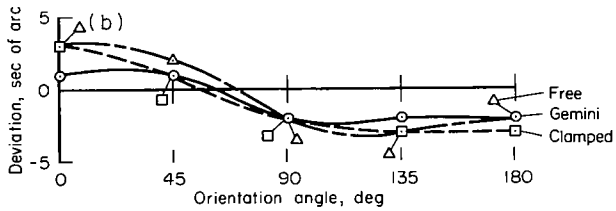

(b) Deviation perpendicular to plane of incidence due to glass subjected to simulation pressure.

Figure 25.- Line-of-sight deviations, aperture C-4, 45° incidence.

clamped edge caused much less deviation in plane, as well as perpendicular to plane of incidence, and also much less cyclic variation. The conclusion can be drawn that the Gemini-type edge condition is quite different from the free- and clamped-edge conditions.

Free- and clamped-edge conditions were used in the study under the assumption that almost all deviation data variations attributable to edge constraint would be encompassed if these constraints were closely simulated. The Gemini-type edge constraint data should then fall within that spectrum of data if the stiffness of the Gemini-type frame were similar to that of the free- and clamped-edge frames so that only the gasketing would enter as a variable. The flatness data of figure 19 showed that the Gemini-type frames were apparently more flexible than the free-edge frames since greater bowing occurred. This greater bowing could lead to the greater deviations experienced. Thus, it can be concluded that, in general, the clamped edge allowed less deviation than the free edge, and that they both allowed less deviation than the Gemini-type frame.

Transmitted Wave Measurements

The distortion to a plane wave front in passing through the three panes of glass was measured for the three types of frames. The distortion to a plane wave contains all the information about the deviation to a line of sight since the direction of an emerging line of sight is perpendicular to this distorted wave at the aperture of interest. The wave-front distortion is an indication of resolution degradation because this distortion causes the loss in resolution. The transmitted wave sums all the effects of lack of flatness, actual wedge, inhomogeneities, etc., and shows their net effect on a flat wave front.

It is apparent from the interferograms of figures 26, 27, and 28 that the window at 15° incidence to the plane wave front, and unbowed by pressure, does not greatly distort a plane wave front and that the edge constraint is not a significant parameter. The fringes are widely spaced and almost straight, indicating that the window acts as a fairly uniform wedge of very small angle. At 45° incidence, there seems to be some effect of edge constraint, but the distortion to the wave front is still very small.

The interferograms of figures 26, 27, and 28 also show the distortion for the same incidence angles but with bowing pressures applied. The distortion at 15° incidence is small and the difference in fringe patterns between the three edge constraints would not significantly change the angle of the wave front at a particular aperture. At 45° incidence, an appreciable difference in the transmitted wave front as a function of edge constraint can be noted. The interferogram of the Gemini-type frame indicates a flat area centrally located on the window with fringes moving out from this area. The free- and clamped-edge frames, however, showed more uniform patterns of fairly straight fringes running across the window as though the plane wave front had changed direction but did not undergo much distortion. The free-edge and the fixed-edge pattern did not differ markedly.

(a) 15° incidence with no pressure.

(b) 15° incidence with simulation pressures.

(c) 45° incidence with no pressure.

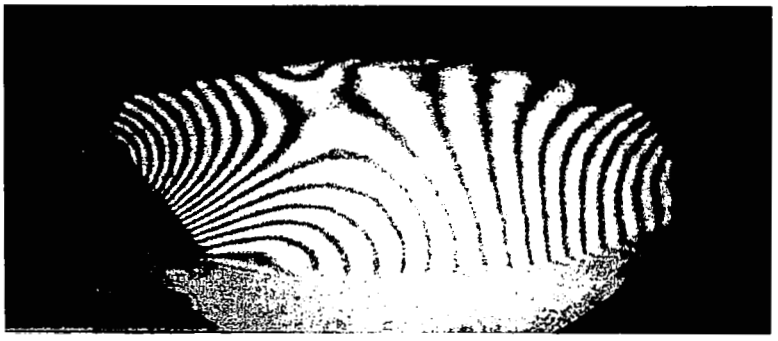

(d) 45° incidence with simulation pressures.

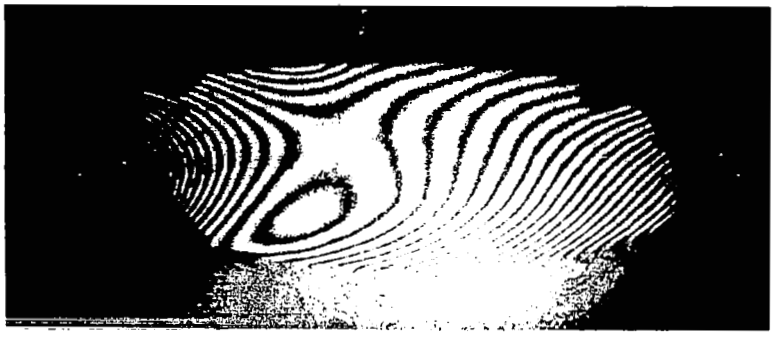

Figure 26.- Transmitted wave interferograms of window in Gemini frames at 90° azimuth angle.

(a) 15° incidence with no pressure.

(b) 15° incidence with simulation pressures.

(c) 45° incidence with no pressure.

(d) 45° incidence with simulation pressures.

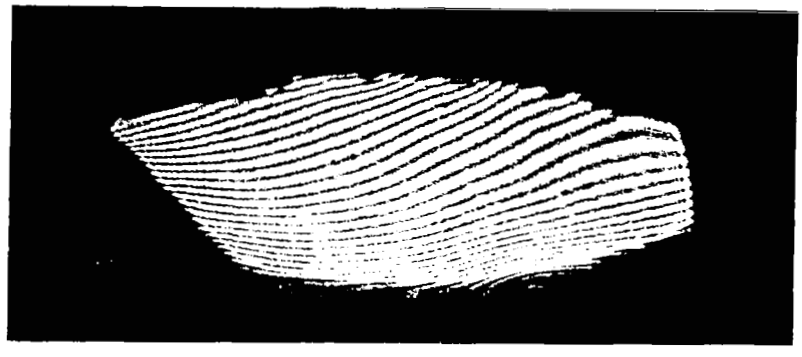

Figure 27.- Transmitted wave interferograms of window in clamped-edge frames at 90° azimuth angle.

(a) 15° incidence with no pressure.

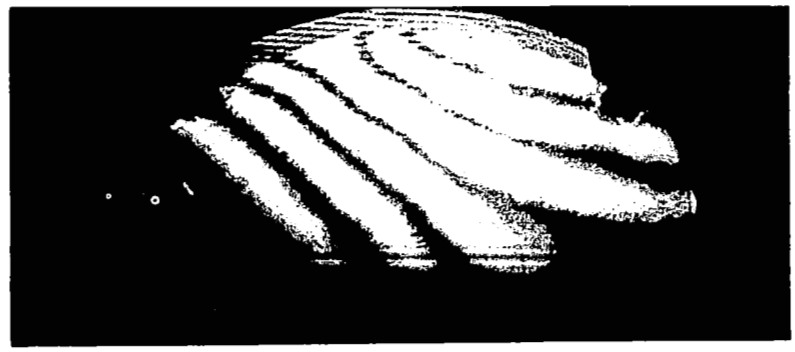

(b) 15° incidence with simulation pressures.

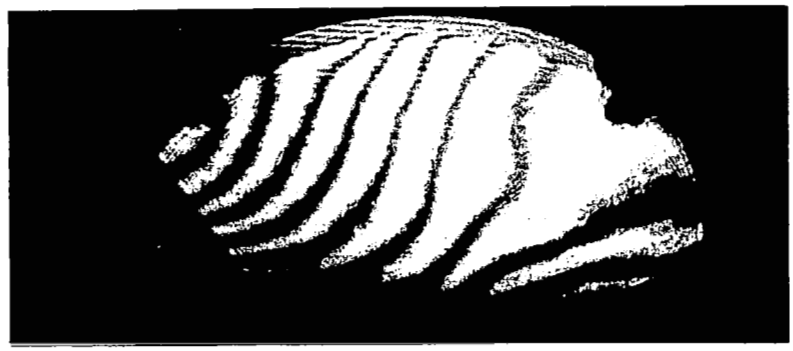

(c) 45° incidence with no pressure.

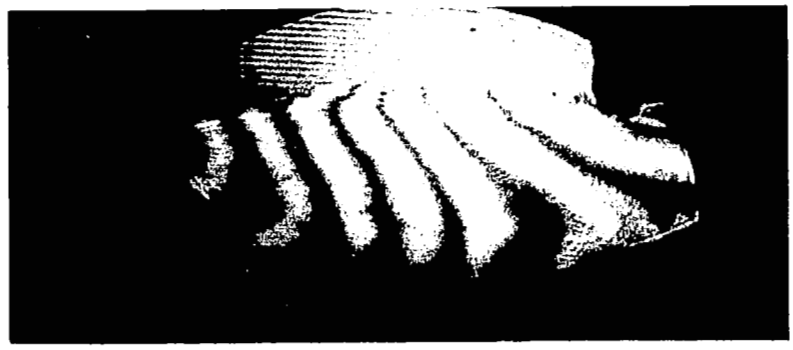

(d) 45° incidence with simulation pressures.

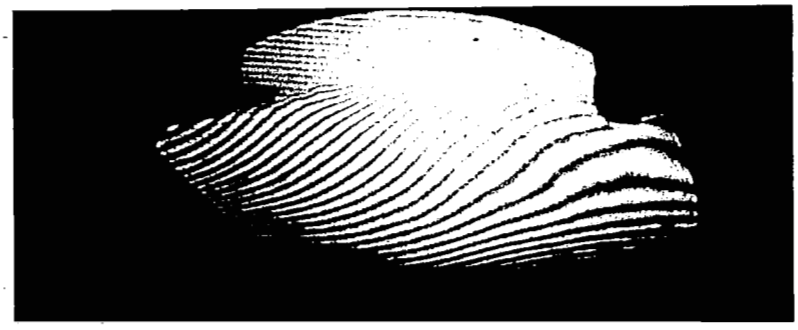

Figure 28.- Transmitted wave interoferograms of window in free-edge frames at 90° azimuth angle.

The transmitted wave interferograms include the contribution of air refraction to the distortion of a plane wave front. The refraction is due to the difference in the refractive index of the air on opposite sides of the inner panes. The interferometer sees a wedge of air when the window is at incidence to the collimated light. The wedge causes the emerging wave front to change direction in the 90° azimuth angle incidence plane. The fringes would be horizontal and evenly spaced in figures 26, 27, and 28 if the glass itself caused no distortion to the wave front.

CONCLUDING REMARKS

The optical measurement system chosen for this study proved to have the necessary versatility and high precision. Measurements of the flatness of the Gemini windows indicated definite contributions of the frames. Without pressure, the Gemini-type frames caused more distortion than either clamped-edge or free-edge frames. With pressure bowing, the Gemini-type frames also permitted more deflection of the panes than either of the other two frames.

Wedge angles measured were below 3 seconds of arc which is small compared to the effects of edge constraints.

The edge constraint effect on resolution was determined to be negligible for an optical system with a 2-inch aperture.

The effect of edge constraint is almost negligible for angles of incidence up to 15°, but at higher incidence the edge constraints affect the windows as a function of plane of incidence, angle of incidence, and aperture location. A clamped-edge constraint caused less deviation to a line of sight than the other two constraints. For the clamped-edge and free-edge constraints, the frame used was a more rigid frame than the Gemini-type frame; this contributed to the smaller deviations.

Because flexing of panes causes significant deviations, thin panes should be avoided in optical quality spacecraft windows and a rigid frame is to be preferred. It can be further surmised that the closer the edge constraint approaches a theoretical fixed edge, the less should be the angular deviations.

Ames Research Center
National Aeronautics and Space Administration
Moffett Field, Calif., 94035, May 29, 1968
125-17-02-13-00-21

REFERENCES

1. Walsh, Thomas M.; Warner, David N., Jr.; and Davis, Michael B.: The Effects of a Gemini Left-Hand Window on Experiments Requiring Accuracy in Sighting or Resolution. NASA TN D-3669, 1966.

2. Silverman, S. M.; and Lloyd, J. W. F.: Optical Environment in Gemini Space Flights. Science, vol. 157, no. 3791, Aug. 25, 1967, pp. 917-919.

3. Forman, Paul F.: The Photographic Window. In: New Development for Aerial Photography, A Program of Talks Presented to Members of OSA, ASP, SPIE, and SPSE at a Joint Technical Meeting, Perkin-Elmer Corp., Electro-Optical Div., Norfolk, Conn., Sept. 16, 1964.

4. Melosh, Robert J.; Diether, Philip A.; and Brennan, Mary: Structural Analysis and Matrix Interpretive System (SAMIS) Program Report. NASA CR-83270, 1966.

TABLE I.- LINE-OF-SIGHT ANGULAR DEVIATION DATA[a]

Angle of incidence, α, deg	Orientation angle, θ, deg	Gemini frames		Clamped-edge frames		Free-edge frames	
		In-plane[b] deviation, $\Delta\alpha$, sec	Out-of-plane[c] deviation, $\Delta\beta$, sec	In-plane[b] deviation, $\Delta\alpha$, sec	Out-of-plane[c] deviation, $\Delta\beta$, sec	In-plane[b] deviation, $\Delta\alpha$, sec	Out-of-plane[c] deviation, $\Delta\beta$, sec
Aperture A-4							
0	0	2	1	1	3	1	3
15	0	7	1	4	-3	4	4
15	45	5	-1	6	0	7	1
15	90	3	-2	4	-2	5	-2
15	135	3	-1	3	-3	3	-3
15	180	4	-2	2	-3	2	-3
30	0	14	3	8	4	8	5
30	45	13	-2	9	-1	12	1
30	90	9	-2	6	-3	9	-4
30	135	10	-1	4	-3	5	-3
30	180	11	-4	5	-3	5	-2
45	0	28	3	14	5	15	8
45	45	25	-4	15	-2	23	0
45	90	20	-3	13	-5	16	-6
45	135	22	1	8	-3	9	-4
45	180	25	-5	9	-2	9	-1
Aperture C-2							
0	0	3	-1	2	2	1	2
15	0	5	-2	2	1	4	2
15	45	4	1	4	0	5	1
15	90	7	-1	4	-2	4	-2
15	135	5	-4	3	-3	2	-2
15	180	0	-3	0	-3	2	-1
30	0	7	-4	3	1	5	3
30	45	4	4	3	1	7	-1
30	90	14	2	5	-1	5	-2
30	135	13	-5	4	-3	5	-1
30	180	5	-7	2	-4	5	-2
45	0	12	-10	2	1	7	5
45	45	3	6	3	1	9	-3
45	90	25	5	5	1	19	-2
45	135	45	-6	9	-2	22	1
45	180	13	-9	6	-4	19	-2

[a]Angular deviation due only to the glass panes when bowed by the simulation pressures.

[b]Component of the angular deviation measured in the plane of incidence.

[c]Component of the angular deviation measured perpendicular to the plane of incidence.

TABLE I.- LINE-OF-SIGHT ANGULAR DEVIATION DATA - Concluded

Angle of incidence, α, deg	Orientation angle, θ, deg	Gemini frames		Clamped-edge frames		Free-edge frames	
		In-plane[b] deviation, $\Delta\alpha$, sec	Out-of-plane[c] deviation $\Delta\beta$, sec	In-plane[b] deviation, $\Delta\alpha$, sec	Out-of-plane[c] deviation, $\Delta\beta$, sec	In-plane[b] deviation, $\Delta\alpha$, sec	Out-of-plane[c] deviation, $\Delta\beta$, sec
Aperture C-4							
0	0	1	2	1	3	1	3
15	0	5	1	3	3	4	3
15	45	6	1	5	1	7	2
15	90	5	-2	5	-2	5	-2
15	135	4	-2	3	-3	3	-3
15	180	3	-2	1	-3	2	-2
30	0	10	2	6	4	8	4
30	45	12	1	7	0	10	0
30	90	10	-3	6	-3	7	-3
30	135	8	-3	4	-3	6	-2
30	180	9	-2	4	-2	6	-2
45	0	20	2	11	3	15	5
45	45	22	0	13	-1	17	-1
45	90	18	-4	9	-3	11	-4
45	135	16	-1	7	-3	11	-2
45	180	19	-2	8	-2	12	-2
Aperture C-6							
0	0	0	2	1	3	1	2
15	0	3	3	2	3	3	3
15	45	6	1	4	1	5	2
15	90	5	-1	4	-2	5	-1
15	135	3	-1	2	-3	3	-2
15	180	4	-1	1	-3	2	-2
30	0	11	5	5	4	6	3
30	45	14	0	8	1	8	1
30	90	9	-4	6	-3	8	-2
30	135	5	-1	3	-3	6	-3
30	180	10	0	2	-3	4	-3
45	0	25	6	12	5	15	4
45	45	29	-2	15	-1	18	0
45	90	15	-7	7	-4	12	-2
45	135	8	1	4	-2	10	-4
45	180	20	2	3	-3	5	-5
Aperture D-4							
0	0	1	1	1	1	1	1
15	0	4	1	3	1	4	2
15	45	5	0	4	-1	4	0
15	90	4	-3	3	-2	3	-2
15	135	2	-2	1	-3	2	-1
15	180	2	-1	1	-2	2	-1
30	0	8	2	5	1	8	2
30	45	10	-1	5	-1	7	-2
30	90	6	-4	3	-3	4	-2
30	135	5	-2	2	-2	4	-1
30	180	8	-1	3	-1	6	-1
45	0	15	2	9	2	14	2
45	45	18	-2	8	-2	12	-3
45	90	9	-6	2	-3	5	-3
45	135	7	1	1	-1	6	1
45	180	17	1	6	0	12	-1

NATIONAL AERONAUTICS AND SPACE ADMINISTRATION
WASHINGTON, D. C. 20546

OFFICIAL BUSINESS

FIRST CLASS MAIL

POSTAGE AND FEES PAID
NATIONAL AERONAUTICS AND
SPACE ADMINISTRATION

POSTMASTER: If Undeliverable (Section 158 Postal Manual) Do Not Return

"The aeronautical and space activities of the United States shall be conducted so as to contribute . . . to the expansion of human knowledge of phenomena in the atmosphere and space. The Administration shall provide for the widest practicable and appropriate dissemination of information concerning its activities and the results thereof."

—NATIONAL AERONAUTICS AND SPACE ACT OF 1958

NASA SCIENTIFIC AND TECHNICAL PUBLICATIONS

TECHNICAL REPORTS: Scientific and technical information considered important, complete, and a lasting contribution to existing knowledge.

TECHNICAL NOTES: Information less broad in scope but nevertheless of importance as a contribution to existing knowledge.

TECHNICAL MEMORANDUMS: Information receiving limited distribution because of preliminary data, security classification, or other reasons.

CONTRACTOR REPORTS: Scientific and technical information generated under a NASA contract or grant and considered an important contribution to existing knowledge.

TECHNICAL TRANSLATIONS: Information published in a foreign language considered to merit NASA distribution in English.

SPECIAL PUBLICATIONS: Information derived from or of value to NASA activities. Publications include conference proceedings, monographs, data compilations, handbooks, sourcebooks, and special bibliographies.

TECHNOLOGY UTILIZATION PUBLICATIONS: Information on technology used by NASA that may be of particular interest in commercial and other non-aerospace applications. Publications include Tech Briefs, Technology Utilization Reports and Notes, and Technology Surveys.

Details on the availability of these publications may be obtained from:

SCIENTIFIC AND TECHNICAL INFORMATION DIVISION

NATIONAL AERONAUTICS AND SPACE ADMINISTRATION

Washington, D.C. 20546